A POLARIZATION-DEPENDENT MULTIBAND RAM DESIGN

X. Yao*, X.-Y. Cao, J. Gao, and Q. Yang

Telecommunication Engineering, Institute of Air Force Engineering University, Xi'an, Shaanxi 710077, China

Abstract—A polarization-dependent mutiband radar absorbing material (PDM-RAM) composed of polarization-dependent multiband AMC (PDMAMC) and perfect electric conductor (PEC) cells is proposed. The PDMAMC is realized by etching a complementary split ring resonator (CSRR) on the patch of a conventional AMC. Around the two/three operational frequencies of the PDMAMC-elements for different electric field polarizations, the reflections of the PDMAMC and PEC have opposite phases, so for any normal incident plane wave the reflections cancel out. The basic principle is discussed, and a sample is measured. The results show that the proposed method is feasible and effective for the polarization-dependent multiband radar cross section (RCS) reduction.

1. INTRODUCTION

Radar cross section (RCS) is a measure of power scattered in a given direction when a target is illuminated by an incident wave. With the developments of the stealth technology and detection technology, the scattering characteristics of a target have received more and more attention. How to reduce the RCS has a great military and practical significance [1, 2].

Metallic arrays, placed over a grounded dielectric substrate, behave as artificial magnetic conductor (AMC) surfaces. They reflect incident waves with zero or near zero phase shifts, for a range of frequencies [3, 4]. This property has been used to design thin radar absorbing materials (RAM), which is a modified design of the Salisbury screen [5] that consists of a lossy resistive sheet placed $\lambda/4$ above a perfect electric conductor (PEC) ground plane. This $\lambda/4$ height

limitation makes the Salisbury screen very bulky at low frequencies. In [6–8], AMC surfaces, which utilize lossy material, have been used to reduce backscatter from the screen. Another way of using AMC surfaces to control the electromagnetic (EM) scattering from targets is based on shaping. The principle is to reflect the EM signals away from the direction of incoming waves. A composite surface of AMC and PEC cells was proposed in [9]. The RCS reduction ability of the composite surface is based on the cancelation of reflection from the interfaces between them. Without using lossy components, the energy is scattered into other directions instead of being absorbed. By controlling the phase difference between the two types of AMC slabs, the RCS along the boresight is reduced over a wide frequency range [10, 11]. This composite surface can be applied to the realization of the in-band RCS reduction of antenna. In [12], a waveguide slot antenna equipped with the ring-shape composite surface is designed to achieve enhanced gain and low in-band RCS simultaneously.

The purpose of this paper is to discuss the performance of the polarization-dependent multiband AMC (PDMAMC) structure constructed by etching a complementary split ring resonator (CSRR) on the patch of a conventional AMC. In addition, a polarization-dependent multiband RAM (PDM-RAM) is proposed based on a combination of PDMAMC and PEC cells in a chessboard like configuration. Similar to the chessboard configuration in [9], the RAM design consists of a new type of AMC, different from the traditional ones, and is designed to satisfy the zero-phase condition at different frequencies. Measured results show good agreement with analyzed and simulated results.

2. PDMAMC DESIGN

The detail of the PDMAMC unit cell by etching a CSRR on the patch of the AMC is shown in Fig. 1. The patch parameters of PDMAMC are the same as the configuration in [13]. It is printed on the PEC-back substrate without vias [14], and the height of which is 2 mm, with a relative permittivity of 2.65. The dimensions of the unit cell are $7.5 \times 7.5 \times 2$ mm. Full wave Floquet's modal analysis has been used to simulate the reflection phase by using Ansoft HFSS 12 [15], assuming plane wave normal incidence. The behaviors of the reflection phase with two resonances (4.36 GHz and 9.75 GHz) for x-polarization (the electric field polarization is kept along the x-axis) and three resonances (3.85 GHz, 4.86 GHz and 7.39 GHz) for y-polarization (the electric field polarization is kept along the y-axis) are shown in Fig. 2.

The electric field distributions for different EM field polarizations
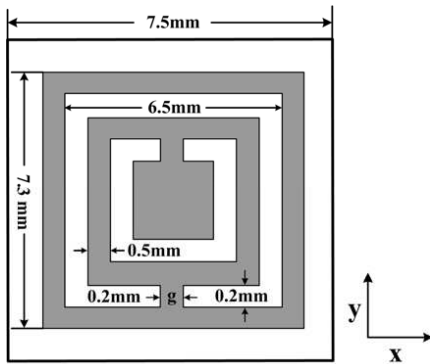
Figure 1. Configuration of the presented PDMAMC unit.
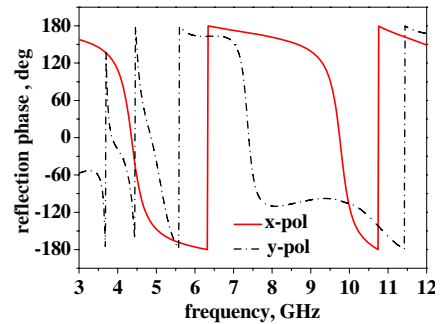
Figure 2. Reflection phase from PDMAMC structure for x-polarization and y-polarization.

are shown in Fig. 3. If the direction of propagation is perpendicular to the CSRR plane and the incident **E** is parallel to the gap-bearing sides of the CSRR [Fig. 3(a)] no coupling to the magnetic resonance is expected. In this case, the CSRR is similar to the dual rings. The patch of PDMAMC mainly contributes to the excitation of the lower resonance frequency whereas the dual rings to that of the higher frequency. If the incident **H** is parallel to the gap-bearing sides of the CSRR [Fig. 3(b)], a magnetic coupling of the incident EM wave to the CSRR occurs. The outer ring mainly contributes to the excitation of the first resonance frequency whereas the inner one to that of the second resonance frequency. In addition, both of the outer and inner rings provide the third resonance frequency [16, 17].

3. PDM-RAM DESIGN

The main idea is based on the design of a surface that reflects the impinging incident wave in phase and counter-phase at the same time, which can be achieved by metallic cells, reflecting incident waves with a $180°$ change of phase, and AMC cells introducing no phase change to the reflected wave at the resonance frequency. Combination of those two contributions leads to destructive interference, achieving a null in boresight direction. The power will be reflected in other directions depending on the design. The combination of these cells is arranged in such a way that any element, PEC or AMC, is surrounded by the other type of element, see Fig. 4(a).

The idea behind the concept can be easily understood by turning to standard array theory [9]. The unit cell can be modeled as a 2×2 antenna array formed by 4 elementary antennas that are assumed to
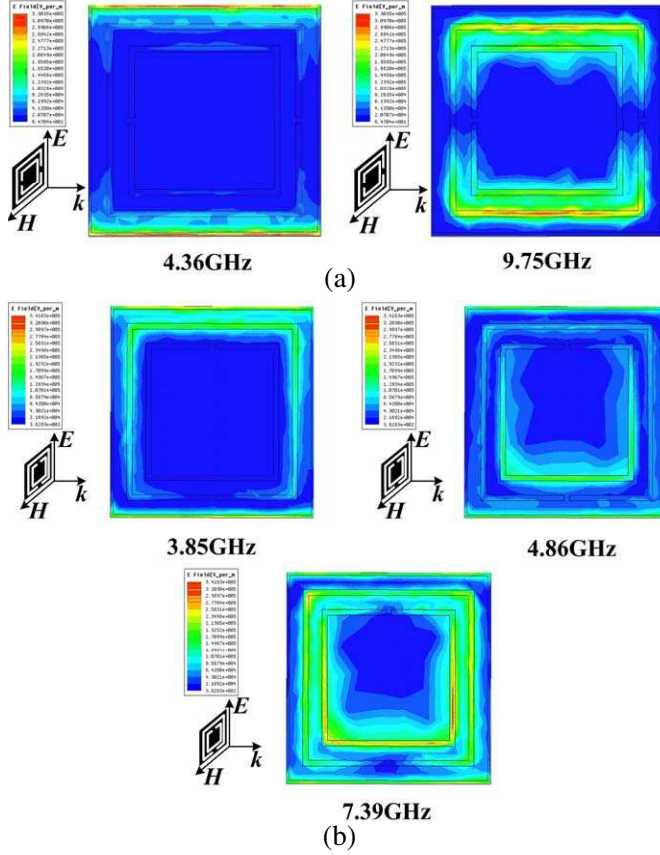
Figure 3. Magnitude distributions of electric field for x-polarization and y-polarization (a) x-polarization at the frequencies of 4.36 GHz and 9.75 GHz, (b) y-polarization at the frequencies of 3.85 GHz, 4.86 GHz and 7.39 GHz.
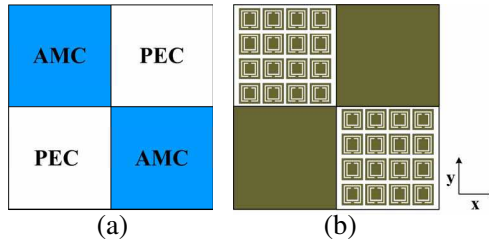
Figure 4. Configuration of the chessboard model and presented PDM-RAM (a) chessboard model (b) presented PDM-RAM.

radiate the same amount of power. However, two of them are in phase and the others in counter-phase. The radiating field of each single elementary antenna is represented by

$$E_{AMC} = A \cdot e^{j \cdot \text{phase}_1} \tag{1}$$

$$E_{PEC} = A \cdot e^{j \cdot \text{phase}_2} \tag{2}$$

in which $\text{phase}_1 \approx 0°$, $\text{phase}_2 \approx 180°$. Then the total field radiated by the array is then simply given by

$$E = E_{AMC} \cdot AF1 + E_{PEC} \cdot AF2 \tag{3}$$

where the array factors are described by the following:

$$AF1 = e^{j(kx+ky)d/2} + e^{j(-kx-ky)d/2} \tag{4}$$

$$AF2 = e^{j(kx-ky)d/2} + e^{j(-kx+ky)d/2} \tag{5}$$

Next, a PDM-RAM is proposed, which utilizes a 4×4 PDMAMC to fill in the AMC area. As the complete chessboard structure is too computationally intensive to be fully modeled, a unit cell configuration based on a 2×2 array as depicted in Fig. 4(b) is analyzed. Element dimensions are fixed to 60×60 mm. Then, we compare the RCS results to those of a PEC plate with comparable dimensions and show monostatic RCS reduction of the frequency dependence of chessboard configuration for normal incidence. The results are done for x and y polarizations [see Fig. 5]. Except for some frequency shift, the two operational frequencies (5.16 GHz, 9.98 GHz) and three operational frequencies (3.98 GHz, 5.02 GHz, 7.66 GHz), of which the RCS have been reduced, agree well with the operational frequencies, around which the effective zero-phase condition is satisfied. The discrepancies are probably because ideal infinite periodic structures are used in the simulations of reflection phase. Since this PDM-RAM presents polarization-dependence and multiband characteristics, the energy impinging upon it is simply redirected for y- and x-polarizations at 7.66 GHz and 9.98 GHz, which show the backscattering characteristics at $\varphi = 0$ cut plane, as may be seen from Figs. 6 and 7, respectively. We can see that the RCS has a reduction of about 27.4 dB and 18.5 dB, respectively. The RCS of RAM is larger than the ones of PEC plate out of the design frequencies because there are no loss components in the composite RAM surface.

4. RESULTS AND ANALYSIS

The whole PDM-RAM sample is 300 mm $\times$ 300 mm in size, i.e., it is a 5×5 array. Also, the reflection coefficients of the sample in Fig. 8 are measured in anechoic chamber using an Agilent N5230C
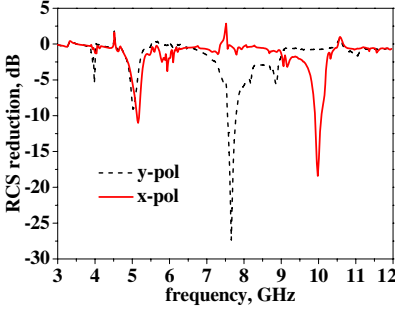
Figure 5. x-polarization and y-polarization RCS reduction as function of the frequency for normal incidence.
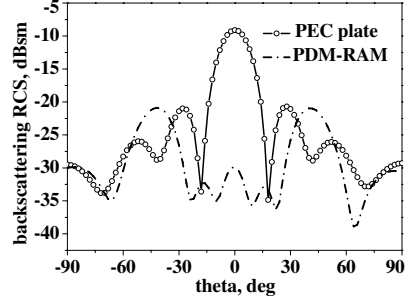
Figure 6. y-polarization backscattering characteristics of PDM-RAM and PEC plate at 7.66 GHz
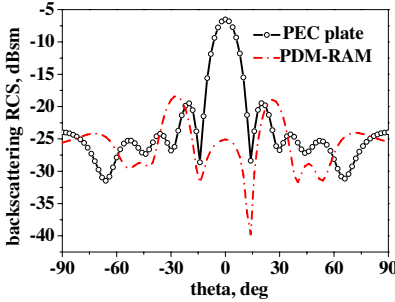
Figure 7. x-polarization backscattering characteristics of PDM-RAM and PEC plate at 9.98 GHz.
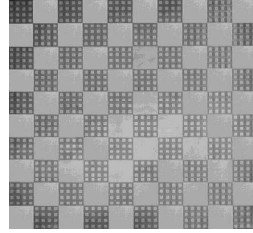
Figure 8. Picture of a PDM-RAM.

network analyzer and microwave horn antenna as shown in Fig. 9. For comparison, the reflection coefficients of a PEC plate of the same size are measured, too [18]. For all measurements, EM waves propagate along the z-direction. The electric field polarization is kept along the x-axis (x-polarization) and y-axis (y-polarization), respectively. Fig. 10 gives the difference of reflection coefficients between PDM-RAM and PEC plate. It is observed that the reflectivity is reduced at least 10 dB around the frequencies (5.48 GHz, 9.8 GHz) for x-polarization and the frequencies (3.86 GHz, 5.61 GHz, 7.05 GHz) for y-polarization. The discrepancies between the measured and simulated results are probably due to the following two reasons: 1) the edge diffraction has effect on the characteristics of the finite PDMAMC structures inside the sample, 2) manufacturing tolerances. It is worth noting that the reflectivity is increased in some frequency bands because of the discrepancies between two measured results and the impedance matching of the horn.
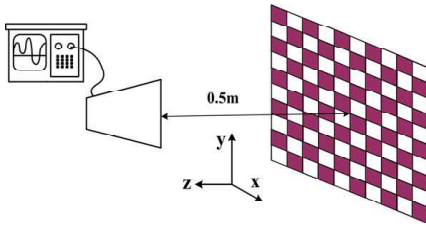
Figure 9. Schematic of the experiment setup.
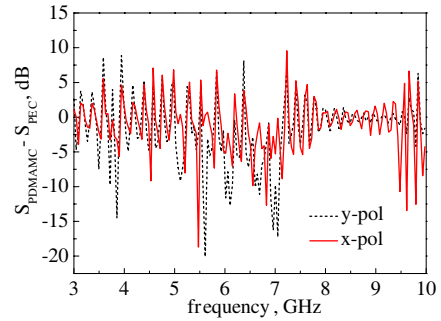
Figure 10. Reflection reduction of the PDM-RAM compared to the reflection from the PEC plate.

5. CONCLUSION

A method for designing PDM-RAM is proposed. It utilizes PDMAMC to redirect the energy and form the boresight and to achieve a reduction in the RCS over a multi-band. The principles of the design are quite simple, and the proposed structure is easy to fabricate.

REFERENCES

1. Ling, J., S.-X. Gong, B. Lu, H.-W. Yuan, W.-T. Wang, and S. Liu, "A microstrip printed dipole antenna with UC-EBG ground for RCS reduction," *Journal of Electromagnetic Waves and Applications*, Vol. 23, Nos. 5–6, 607–616, 2009.

2. Wang, W.-T, S.-X. Gong, Y.-J. Zhang, F.-T. Zha, J. Ling, and T. Wan, "Low RCS dipole array synthesis based on MOM-PSO hybrid algorithm," *Progress In Electromagnetics Research*, Vol. 94, 119–132, 2009.

3. Sievenpiper, D., et al., "High-impedance electromagnetic surfaces with a forbidden frequency band," *IEEE Trans. on Microw. Theory and Tech.*, Vol. 47, 2059–2074, 1999.

4. Goussetis, G., A. P. Feresidis, and J. C. Vardaxoglou, "Tailoring the AMC and EBG characteristics of periodic metallic arrays printed on grounded dielectric substrate," *IEEE Trans. on Antennas and Propag.*, Vol. 54, No. 1, 82–89, 2006.

5. Fante, R. L. and M. T. McCormack, "Reflection properties of the Salisbury screen," *IEEE Trans. on Antennas and Propag.*, Vol. 36, No. 10, 1443–1454, 1988.

6. Gao, Q., Y. Yin, D. B. Yan, and N. C. Yuan, "Application of metamaterials to ultra-thin radar-absorbing material design," *Electron. Lett.*, Vol. 41, No. 17, 936–937, 2005.

7. Simms, S. and V. Fusco, "Tunable thin radar absorber using artificial magnetic ground plane with variable backplane," *Electron. Lett.*, Vol. 42, No. 21, 1197–1198, 2006.

8. Costa, F., A. Monorchio, and G. Manara, "Analysis and design of ultra thin electromagnetic absorbers comprising resistively loaded high impedance surfaces," *IEEE Trans. on Antennas and Propag.*, Vol. 58, No. 5, 1551–1558, 2010.

9. Paquay, M., J. C. Iriarte, I. Ederra, R. Gonzalo, and P. de Maagt, "Thin AMC structure for radar cross-section reduction," *IEEE Trans. on Antennas and Propag.*, Vol. 55, No. 12, 3630–3638, 2007.

10. Zhang, Y., R. Mittra, B. Z. Wang, and N. T. Huang, "AMCs for ultra-thin and broadband RAM design," *Electron. Lett.*, Vol. 45, No. 10, 484–485, 2009.

11. Fu, Y. Q., Y. Q. Li, and N. C. Yuan, "Wideband composite AMC surfaces for RCS reduction," *Microw. Opt. Technol. Lett.*, Vol. 53, No. 4, 712–715, 2011.

12. Tan, Y., N. Yuan, Y. Yang, and Y. Fu, "Improved RCS and efficient waveguide slot antenna," *Electron. Lett.*, Vol. 47, No. 10, 582–583, 2011.

13. Peng, L., C. L. Ruan, and Z. Q. Li, "A novel compact and polarization-dependent mushroom-type EBG using CSRR for dual/triple-band applications," *IEEE Microw. Wireless Compon. Lett.*, Vol. 20, No. 9, 489–491, 2010.

14. Hosseini, M, A. Pirhadi, and M. Hakkak, "A novel AMC with little sensitivity to the angle of incidence using 2-layer Jerusalem cross FSS," *Progress In Electromagnetics Research*, Vol. 64, 43–51, 2006.

15. Ansoft HFSS ver. 12, www.Ansoft.com

16. Katsarakis, N., T. Koschny, and M. Kafesaki, "Electric coupling to the magnetic resonance of split ring resonators," *Appl. Phys. Lett.*, Vol. 84, No. 15, 2943–2945, 2004.

17. Falcone, F., T. Lopetegi, and J. D. Baena, "Effective negative-ε stopband microstrip lines based on complementary split ring resonators," *IEEE Microw. Wireless Compon. Lett.*, Vol. 14, No. 6, 280–282, 2004

18. Liu, Y. C., C. Y. Liu, and C. P. Kuei, "Design and analysis of broadband microwave absorber utilizing FSS screen constructed with circular fractal configurations," *Microw. Opt. Technol. Lett.*, Vol. 48, No. 3, 449–453, 2005.